

Research Article

Interactive Echocardiography Translation Using Few-Shot GAN Transfer Learning

Long Teng ¹, ZhongLiang Fu,¹ Qian Ma,² Yu Yao,¹ Bing Zhang,² Kai Zhu,¹ and Ping Li³

¹Chengdu Institute of Computer Application, University of Chinese Academy of Sciences, Beijing, China

²Sichuan University of Media and Communications, Chengdu, China

³West China Hospital, Sichuan University, Chengdu, China

Correspondence should be addressed to Long Teng; 52867567@qq.com

Received 9 July 2019; Revised 19 January 2020; Accepted 17 February 2020; Published 19 March 2020

Guest Editor: Andrea Duggento

Copyright © 2020 Long Teng et al. This is an open access article distributed under the Creative Commons Attribution License, which permits unrestricted use, distribution, and reproduction in any medium, provided the original work is properly cited.

Background. Interactive echocardiography translation is an efficient educational function to master cardiac anatomy. It strengthens the student's understanding by pixel-level translation between echocardiography and theoretically sketch images. Previous research studies split it into two aspects of image segmentation and synthesis. This split makes it hard to achieve pixel-level corresponding translation. Besides, it is also challenging to leverage deep-learning-based methods in each phase where a handful of annotations are available. **Methods.** To address interactive translation with limited annotations, we present a two-step transfer learning approach. Firstly, we train two independent parent networks, the ultrasound to sketch (U2S) parent network and the sketch to ultrasound (S2U) parent network. U2S translation is similar to a segmentation task with sector boundary inference. Therefore, the U2S parent network is trained with the U-Net network on the public segmentation dataset of VOC2012. S2U aims at recovering ultrasound texture. So, the S2U parent network is decoder networks that generate ultrasound data from random input. After pretraining the parent networks, an encoder network is attached to the S2U parent network to translate ultrasound images into sketch images. We jointly transfer learning U2S and S2U within the CGAN framework. Results and conclusion. Quantitative and qualitative contrast from 1-shot, 5-shot, and 10-shot transfer learning show the effectiveness of the proposed algorithm. The interactive translation is achieved with few-shot transfer learning. Thus, the development of new applications from scratch is accelerated. Our few-shot transfer learning has great potential in the biomedical computer-aided image translation field, where annotation data are extremely precious.

1. Background

Echocardiography education has dramatically helped students to master cardiac structure assessment by combining cardiac ultrasound images with simulators. However, a more efficient method of interactive translation between ultrasound images and theoretically sketch images is still lacking. This causes the image processing difficulties in our case: echocardiography is characterized by the deformable appearance and poor spatial resolution, while limited annotations are available, building obstacles to achieve good performance as well as leverage state-of-the-art deep learning methods.

U2S and S2U are often investigated in different approaches. U2S is often specified in the segmentation task. It is addressed with the following methods: Level set (LS) [1] segmentation,

Deformable templates [2, 3], Active shape models (ASM) [4, 5], Active contour methods, Active appearance models (AAM), Bottom-up approaches, and Database-guided (DB-guided) segmentation. LS and deformable templates present some drawbacks regarding the prior knowledge included in the optimization function. Active contour methods inspire the development of level set (LS) methods. ASM- and DB-guided approaches require a large number of annotated training images [6]. Bottom-up approaches are sensitive to initial conditions and lack of robustness. Additionally, none of those approaches are used to infer the sector boundary, which is essential for comprehension during education.

S2U typically models the tissue response as a collection of point scattering centers [7]. Different amplitudes are assigned to scatter from the blood pool or muscle. However,

due to ignoring surrounding conditions like papillary muscles, clutter noise, and local intensity variations, the genuineness of the synthetic ultrasound images is still unsatisfactory. Some improvements in combining ultrasound recording as a template to synthetic realistic speckle textures are proposed to address the above issue [8, 9]. However, those approaches unavoidably introduced unrealistic warping in simulated speckle texture.

GAN-based translation approach recently shows its potential in generative applications [10]. Structure [11] and texture [12, 13] generation are explored in different applications. While giving an outstanding performance, the GAN approach requires sufficient annotation, which is time-consuming and expensive for biomedical applications.

In this paper, we design a GAN-based transfer learning framework to interactively translate ultrasound images into sketch images (U2S translation) and sketch images into ultrasound images (S2U translation) with a handful of annotations. Figure 1 shows the example results of final U2S translation and S2U translation.

2. Methods

Our approach of interactive translation consists of two steps: pretrain U2S parent network and S2U parent network and train the two networks together with end-to-end transfer learning.

Transfer learning is used for fast adaption and avoiding overfitting since we got only a handful of annotations. In our case, parent networks are carefully designed and pretrained with supervised and unsupervised learning. GAN-based few-shot transfer learning is then designed to fine-tuning the final result.

The proposed U2S network (Figure 2) contains a parent network that follows the U-net [14] architecture. In this paper, the U-net structure contains 10 block layers. The first five blocks are convolutional downsampling networks. Kernel size here is 3, the stride is 2, and padding is 1. Each layer is followed by a batch norm layer and a relu layer. Correspondingly, the last five layers are deconvolutional upsampling networks. Its kernel size is 4, the stride is 2, and padding is 1. The batch norm and relu layer are also adopted. Skip-connection is realized by a concatenate layer between the symmetrical layers. U2S parent network is pretrained on VOC2012 dataset [15]. During the pretraining process, the loss function is class-balanced cross-entropy.

When U2S parent network is ready, we would then transfer the U2S Parent Network into sketch translation. The Conditional Generative Adversarial Network (CGAN) [16] framework is chosen here during transfer learning to infer sector boundary. Now, the U2S Parent Network is regarded as the generation network part of CGAN. It translates ultrasound images into sketch images. The CGAN framework could intuitively generate sketch images with sector boundaries. Also, we add L1 loss as an optional criterion.

$$L_S = -E[\log[D_S(S, U)]] - E[\log[1 - D_S(G_S(U), U)]] + L_{l1}. \quad (1)$$

In equation (1), D_S is the discriminator. It contains 5 block layers. Block layers contain convolution, batch normalization, and relu layers. D_S determines whether the input image is translated data or ground truth. S represents the ground truth sketch image. U represents ground truth ultrasound image. G_S is the generator (initialized with U2S Parent Network). It translates the ultrasound image into a sketch image.

S2U recovers the ultrasound texture from the sketch. Sketch image contains only the structure and no texture information at all. We first extract and maintain texture within the parent network and then synthesis texture on the specific sketch.

As shown in Figure 3, the S2U Parent Network is the decoder network. Our approach trains GAN to generate an ultrasound image on the condition of random input. In this way, as the generator part of GAN, the S2U Parent Network learns the ultrasound texture from training dataset. The S2U Parent Network consists of 4 block layers. The first 3 blocks contain a deconvolution layer, a batch normalization layer, and a relu layer. The last block contains a deconvolution layer and a tanh layer.

The S2U Parent Network training phase is shown in Figure 4. The generator and discriminator loss graphs are listed in the second row. The result of S2U Parent Network is illustrated in the first row. The generator and discriminator play against each other. As a result, the generator learns a growing quality of ultrasound textures.

When S2U Parent Network is ready, we could move forward to S2U transfer learning. Till now, our S2U Parent Network still has two flaws. Firstly, it cannot generate an ultrasound image on the condition of sketch input, not even pixel-level translation. Secondly, unexpected twist and image blur occur in Ultrasound Parent Network.

Aiming at making up for those two flaws, we further reform the network into S2U architecture that is shown in Figure 5. Pretrained S2U Parent Network is the dark blue part. An encoder network marked in light blue is connected to S2U Parent Network. This connection enables generation from a sketch to ultrasound image, other than from random initialization. In fact, the encoder network turns sketch image into the subset of random input. Thus, transfer learning learns the pixel-wise corresponding translation between sketch and ultrasound images. Besides, perceptual loss [17] and total variation loss are attached to the loss function. We try to maximize the fidelity of spatial resolution by minimizing GAN loss and perceptual loss. The loss function is shown in

$$L_U = -E[\log[D_U(U, S)]] - E[\log[1 - D_U(G_U(S), S)]] + \lambda_1 L_{\text{pct}} + \lambda_2 L_{\text{TV}} + \lambda_3 L_{l1}. \quad (2)$$

Intuitively, the loss function of S2U is similar to equation (1). D_U is discriminator. It determines whether the input image is synthesized by the network, or comes from the ground truth. D_U has 5 block layers and is shown in Figure 5. U represents ultrasound ground truth. G_U is the generator

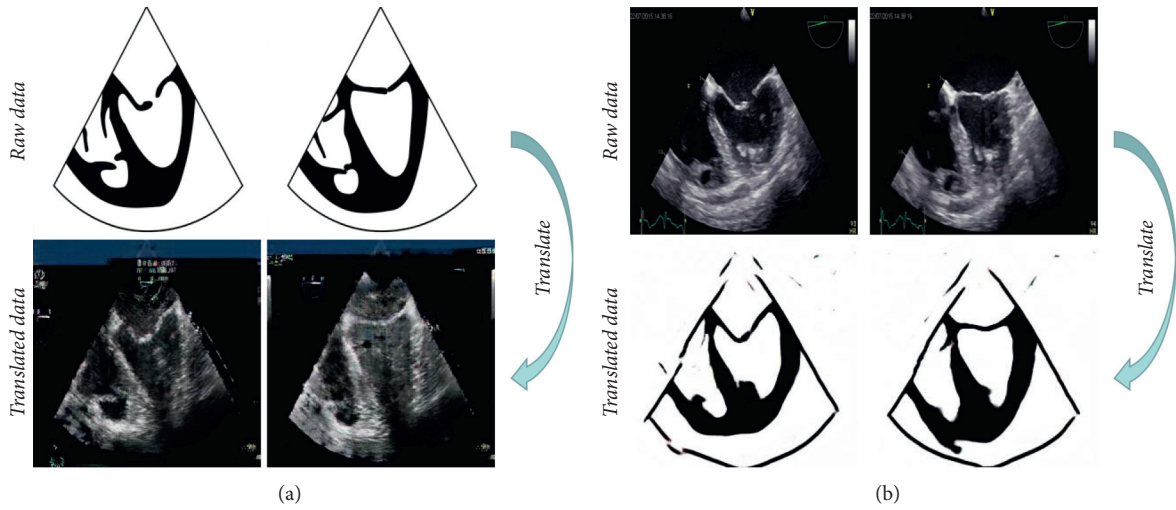


FIGURE 1: Example of interactive translation. The first two columns illustrate (a) S2U translation and the last two columns illustrate (b) U2S translation.

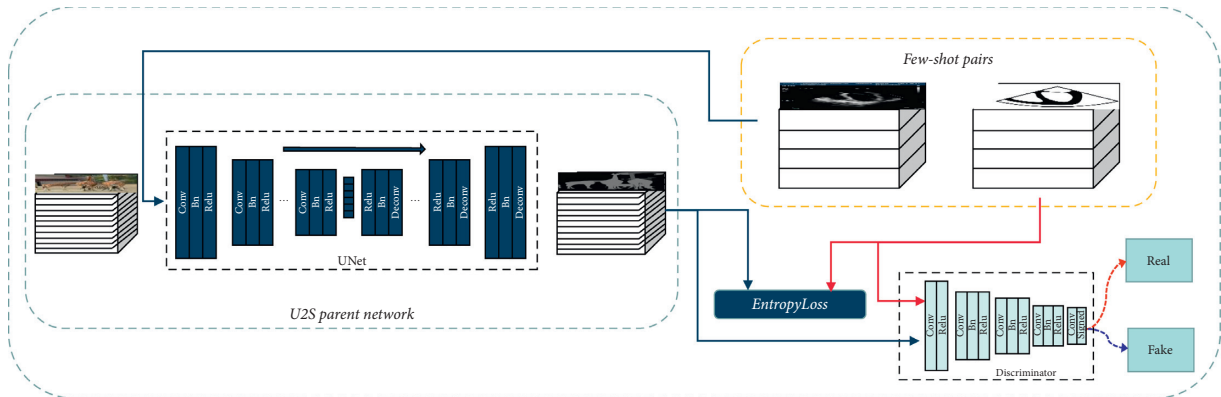


FIGURE 2: U2S network.

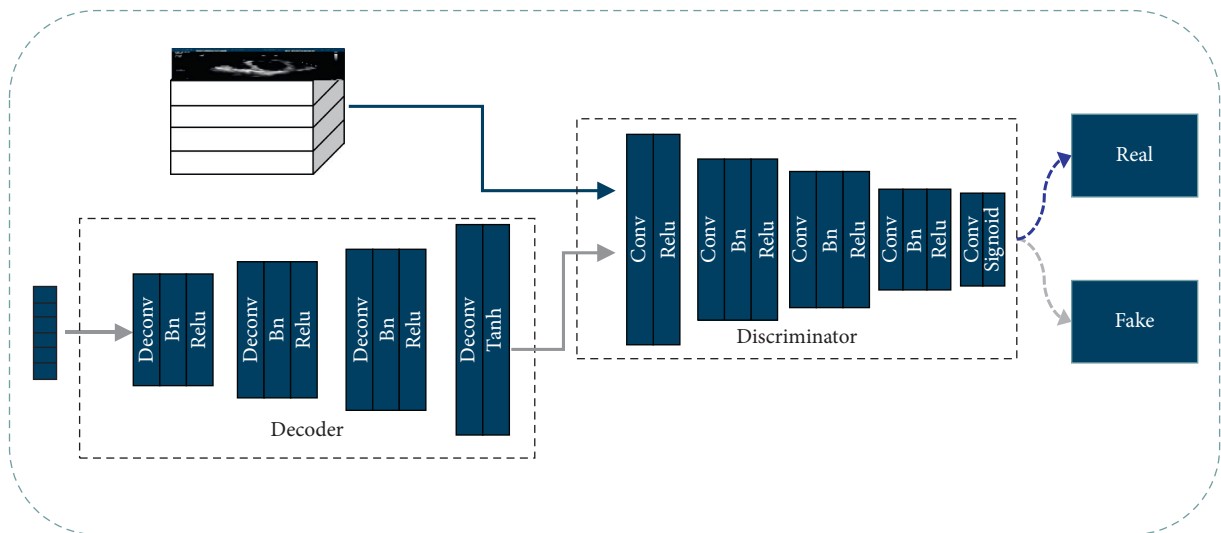


FIGURE 3: S2U Parent Network.

pairs. In Figures 2 and 4, we emphasized this similarity by marking the yellow dash blocks.

Therefore, we integrate U2S and S2U for interactive translation.

$$L_{\text{total}} = L_S + L_U. \quad (3)$$

During transfer learning, the S2U network is trained with TVL1 loss, perceptual loss, L1 loss, and CGAN loss to maintain ultrasound texture. After transfer learning for both two networks, each network splits into the following interactive application (Figure 6 shows our applications).

2.1. Interactive U2S Translation. In some scenarios, the student would carefully study the static picture that captured in dynamic echo video. During this interaction, the local area should be amplified and translated into a sketch at a breakneck speed. Otherwise, the interaction would get stuck and result in a terrible experience.

In this paper, we complete sketch translation at the start of the interaction. Region of interest (ROI) is then selected and amplified to the size of the original image. Notice that, sketch image is the black-and-white image, cubic interpolation is chosen for amplification. The cubic interpolation is efficient and enough for identification.

2.2. Video U2S Translation. During training, automatic U2S translation would greatly help students to comprehend. Here, we split the U2S Network part from the whole networks. U2S network inputs ultrasound images and outputs sketch images. So every frame is translated into sketch images. We process frame-by-frame, converting all frames into a video. This translated sketch video is dynamically contrast to echocardiography to illustrate structural information.

2.3. Interactive S2U Translation. If the student draws a sketch, which outlines the cardiac structure, how the sketch corresponds to the clinical ultrasound image? This interaction could be thought-provoking and, in turn, help for comprehension.

We extract the decoder network in the S2U Parent Network and turn it into an S2U network with an encoder network. S2U inputs sketch and outputs an ultrasound image. It strictly generates output with an appropriate ultrasound texture. So, after students complete their sketch in the drawing board, the sketch image could interactively be translated into an ultrasound image.

3. Results

In this section, we compare the method of U2S translation and S2U translation with 1-shot, 5-shot, and 10-shot transfer learning. Firstly, the performance is analyzed through the visual comparison and the visualization of transfer learning process. Then, the performance is investigated through numerical comparison. In numerical comparison, each experiment is summarized through 45 pairs of annotations.

Besides, we supplement S2U translation performance with and without perceptual loss and TVL1 loss during numerical comparison.

3.1. Dataset. Two datasets are used in this paper, VOC2012 and echocardiography dataset. VOC2012 is an open access segmentation dataset used for the pretraining of the U2S parent network. The echocardiography dataset is collected in the hospital under the guidance of doctors. It contains 5152 four-chamber view echocardiographs with no annotation, and 55 pairs of annotated four-chamber view echocardiographs (in this paper, we use 10 pairs for training and left 45 pairs of the annotated images for validation). Those annotations are made by the teamwork of doctors and art teachers. Images are fully annotated with the chamber (atrial and ventricular), sector boundary, and myocardial. Sensitive patient information is manually removed.

3.2. Visual Comparison. A pair of validation images is chosen to analyze the performance of our proposed network. As shown in Figure 7, the left column is a pair of ground truth. The first row shows S2U results from 1-shot, 5-shot, and 10-shot. The contrast between myocardium and chamber is getting obvious while inputting more transfer learning data. Also, the image resolution is getting better, which makes the myocardium more realistic.

Compared with the real ultrasound images, the S2U results' texture is more similar to the training data. The blue bar and some comments from training data are synthesized on S2U results. In the second row, 1-shot, 5-shot, and 10-shot results of U2S are shown in order. The shape of the U2S result is getting similar to the ground truth. The sector boundary of U2S is also getting reasonable with more training data.

3.3. Transfer Learning Process. The performance of transfer learning process is investigated in two aspects, the loss function value and the corresponding performance during training. The loss function value of S2U and U2S is a representative, shown with 5-shot in Figure 8.

As is shown in Figure 8, the first row is the first three terms of L_U , and the second row is the terms of L_S . The discriminator and generator loss of S2U and U2S are the first two images in the first and second rows. In both S2U and U2S, the generator and discriminator contest against each other, while the perceptual loss of S2U and the L1 loss of U2S keep decreasing. The adversarial loss function and extra loss function work together to fine-tune the final result. Figure 9 shows the performance on testing data.

In Figure 9, the Intersection over Union (IOU) and peak signal to noise ratio (PSNR) result are representatively illustrated in 1-shot, 5-shot, and 10-shot. As a result of the proposed loss function, S2U and U2S achieve improving performance during training. Specifically, the more the training samples, the better the performance achieved. 10-shot transfer learning achieves better performance than 5-shot, while 5-shot achieves better performance than 1-shot.

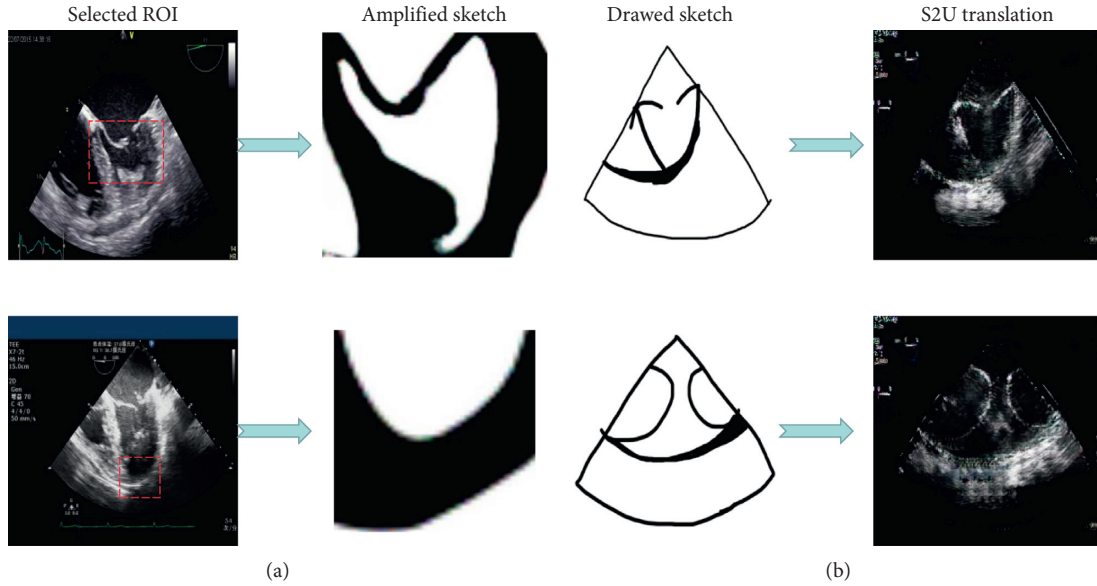


FIGURE 6: Interactive translation applications. First two columns illustrate interactive (a) U2S translation and last two columns illustrate interactive (b) S2U translation.

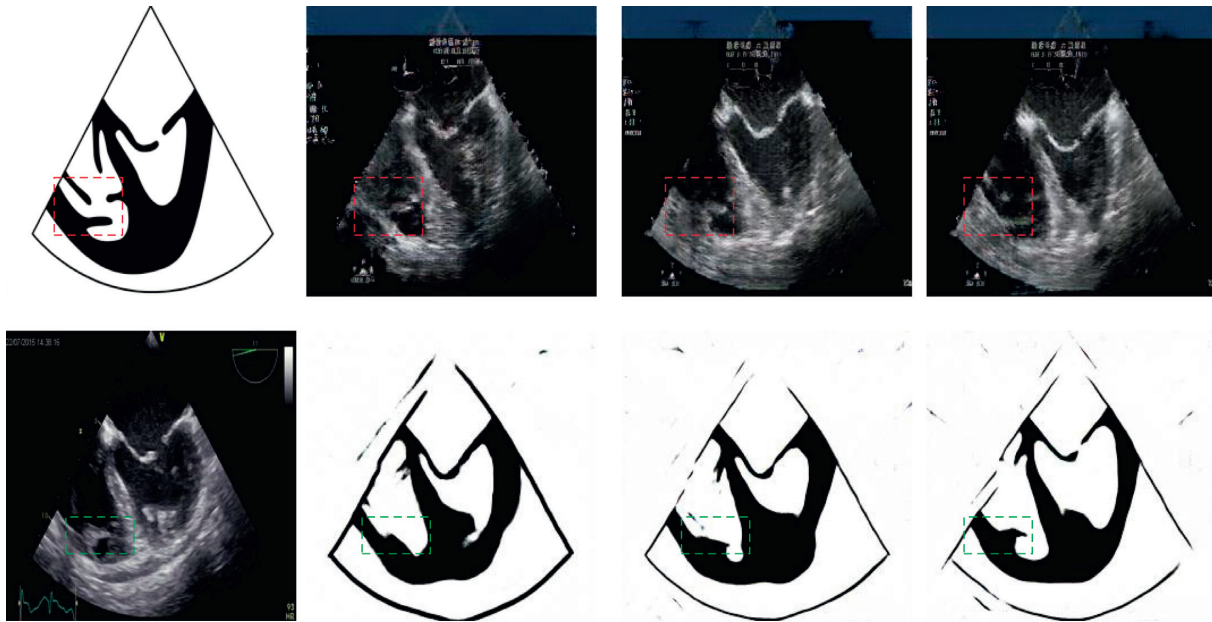


FIGURE 7: Example performance of few-shot transfer learning. The first row shows S2U of 1-shot, 5-shot, and 10-shot; the second row shows U2S of 1-shot, 5-shot, and 10-shot. The left column is a pair of ground truth.

3.4. Numerical Comparison. In U2S translation, we adopt the medical image segmentation index of dice loss, volumetric overlap error (VOE), and intersection over union (IOU). In S2U translation, we use peak signal to noise ratio (PSNR) and structural similarity index (SSIM) to evaluate our performance.

The convincing result below (Tables 1 and 2) shows the effectiveness of proposed few-shot transfer learning with

1-shot, 5-shot, and 10-shot. In Table 1, the gradual increase of training samples leads to better performance of the index. In Table 2, the indexes of PSNR and SSIM are compared with and without extra loss function.

As is shown in Table 1, few-shot learning has led to acceptable results in all of the indexes. It enables us to present the initial version of the U2S function while lacking annotations.

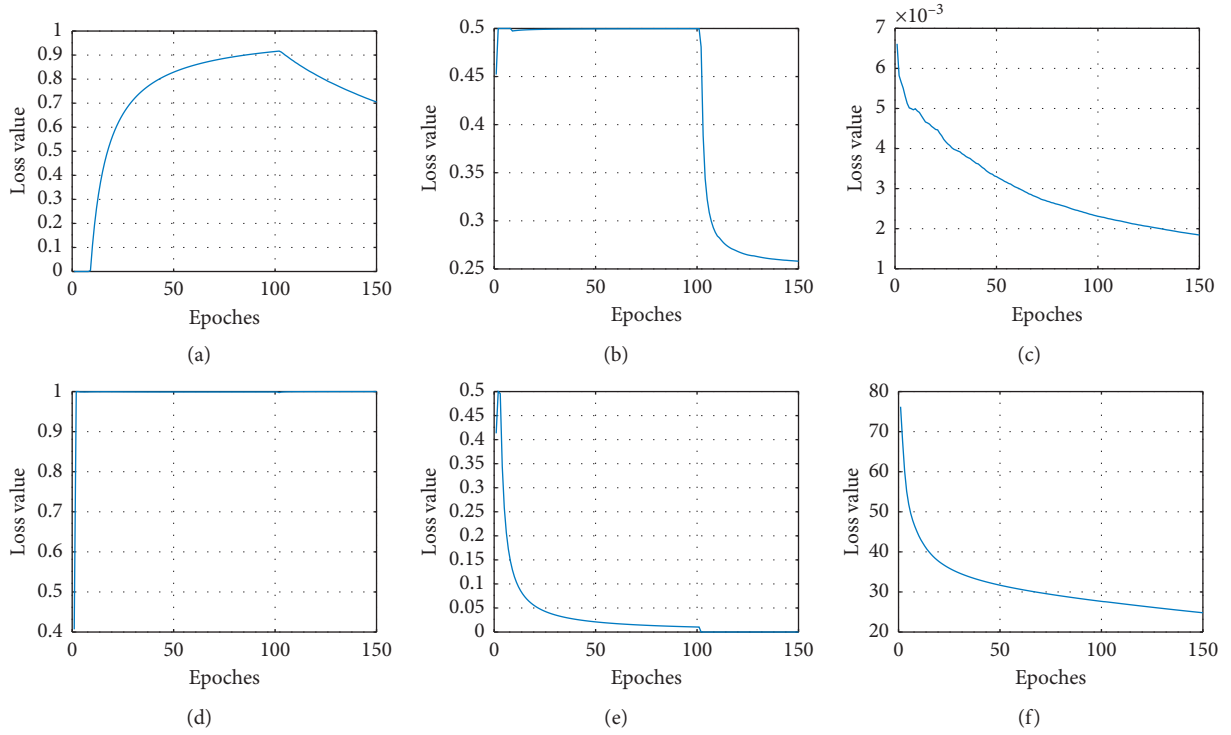


FIGURE 8: Loss function value during transfer learning. The S2U and U2S loss value during transfer learning. (a) S2U generator loss. (b) S2U discriminator loss. (c) S2U generator perceptual loss. (d) U2S generator loss. (e) U2S discriminator loss. (f) S2U generator L1 loss.

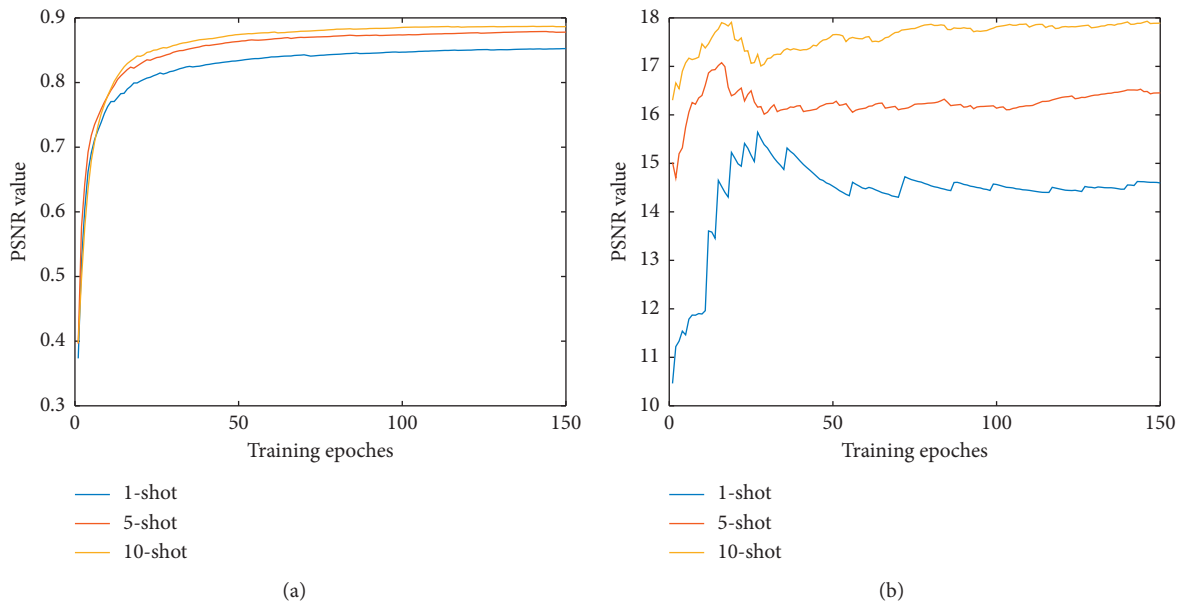


FIGURE 9: U2S and S2U performance during transfer learning. The IOU index of U2S and the PSNR index of S2U during transfer learning. (a) IOU—few-shot transfer learning. (b) PSNR—few-shot transfer learning.

TABLE 1: U2S translation accuracies on our dataset.

U2S	DICE	VOE	IOU
1-shot	0.902	0.001	0.852
5-shot	0.913	0.018	0.872
10-shot	0.921	-0.009	0.887

TABLE 2: S2U translation accuracies on our dataset.

S2U	PSNR	PSNR (No. perceptual and TVL1 loss)	SSIM	SSIM (No. perceptual and TVL1 loss)
1-shot	14.614	14.898	0.417	0.406
5-shot	16.180	16.074	0.499	0.433
10-shot	17.905	17.575	0.544	0.553

According to the result of Table 2, S2U that trained with the perceptual and TVL1 loss is generally better without those loss functions.

4. Conclusion

This paper proposed a few-shot GAN Transfer Learning for Interactive Echocardiography Translation. U2S Parent Network and S2U Parent Network are individually designed and pretrained beforehand. Then, they are assembled together for transfer learning. This joint transfer learning transfers prior knowledge into target networks. Qualitative analysis of visual comparison and visualization of the transfer learning process, quantitative analysis of numerical index shows the effectiveness of the proposed method.

The proposed method has two advantages over previous researches. Firstly, it simultaneously achieves interactive translation between ultrasound and sketch images with few-shot annotations, enabling a new educational interactive function before getting enough annotation. Secondly, it is also promising in further improvement with more training data and is promising in other related biomedical applications.

Data Availability

Part of our dataset used in the current study is available from the corresponding author on a reasonable request. Our code is open source at: <https://github.com/tlok666/Interactive-Echocardiography-Translation-with-Few-Shot-GAN>.

Ethical Approval

This study was approved by the Medical Ethics Committee of the West China Hospital, Sichuan University, and written informed consent was obtained from each participant.

Conflicts of Interest

The authors declare no conflicts of interest.

Authors' Contributions

Long Teng contributed equally to this work. Long Teng, ZhongLiang Fu, and Kai Zhu designed the research. Long Teng completes all the code and paper material. Qian Ma, Bing Zhang, and Ping Li prepared the dataset. Yu Yao is responsible for the application of the proposed algorithm.

Acknowledgments

The authors would like to thank to the doctors in the Department of Anesthesiology, West China Hospital, Sichuan

University, for their helpful contribution with collecting and validating the data. This study was supported by Sichuan Province's New Generation of Artificial Intelligence Major Special Project (Grant no. 2018GZDZX0036).

References

- [1] S. Mazaheri, P. S. B. Sulaiman, R. Wirza et al., "Echocardiography image segmentation: a survey," in *Proceedings of the 2013 International Conference on Advanced Computer Science Applications and Technologies*, pp. 327–332, Kuching, Malaysia, December 2013.
- [2] K. Chauhan and R. Chauhan, "Boundary detection of echocardiographic images during mitral regurgitation," in *Recent Advances in Computer Vision*, pp. 281–303, Springer, Berlin, Germany, 2019.
- [3] G. Veni, M. Moradi, H. Bulu, G. Narayan, and T. Syeda-Mahmood, "Echocardiography segmentation based on a shape-guided deformable model driven by a fully convolutional network prior," in *Proceedings of the 2018 IEEE 15th International Symposium on Biomedical Imaging (ISBI 2018)*, pp. 898–902, Washington, DC, USA, April 2018.
- [4] T. F. Cootes, C. J. Taylor, D. H. Cooper, and J. Graham, "Active shape models-their training and application," *Computer Vision and Image Understanding*, vol. 61, no. 1, pp. 38–59, 1995.
- [5] S. C. Mitchell, B. P. F. Lelieveldt, R. J. Van Der Geest, H. G. Bosch, J. H. C. Reiver, and M. Sonka, "Multistage hybrid active appearance model matching: segmentation of left and right ventricles in cardiac mr images," *IEEE Transactions on Medical Imaging*, vol. 20, no. 5, pp. 415–423, 2001.
- [6] S. Leclerc, E. Smistad, J. Pedrosa et al., "Deep learning for segmentation using an open large-scale dataset in 2d echocardiography," *IEEE Transactions on Medical Imaging*, vol. 20, 2019.
- [7] M. Alessandrini, M. De Craene, O. Bernard et al., "A pipeline for the generation of realistic 3d synthetic echocardiographic sequences: methodology and open-access database," *IEEE Transactions on Medical Imaging*, vol. 34, no. 7, pp. 1436–1451, 2015.
- [8] A. Prakosa, M. Sermesant, H. Delingette et al., "Generation of synthetic but visually realistic time series of cardiac images combining a biophysical model and clinical images," *IEEE Transactions on Medical Imaging*, vol. 32, no. 1, pp. 99–109, 2012.
- [9] S. Marchesseau, H. Delingette, M. Sermesant et al., "Preliminary specificity study of the Bestel-Clément-Sorine electromechanical model of the heart using parameter calibration from medical images," *Journal of the Mechanical Behavior of Biomedical Materials*, vol. 20, pp. 259–271, 2013.
- [10] P. Isola, J.-Y. Zhu, T. Zhou, and A. A. Efros, "Image-to-image translation with conditional adversarial networks," in *Proceedings of the IEEE Conference on Computer Vision and Pattern Recognition*, pp. 1125–1134, Honolulu, HI, USA, July 2017.

- [11] B. Chang, Q. Zhang, S. Pan, and L. Meng, "Generating handwritten Chinese characters using cyclegan," in *Proceedings of the 2018 IEEE Winter Conference on Applications of Computer Vision (WACV)*, pp. 199–207, Lake Tahoe, NV, USA, March 2018.
- [12] C. Chu, A. Zhmoginov, and M. Sandler, "Cyclegan, a master of steganography," 2017.
- [13] J.-Y. Zhu, T. Park, P. Isola, and A. A. Efros, "Unpaired image-to-image translation using cycle-consistent adversarial networks," in *Proceedings of the IEEE International Conference on Computer Vision*, pp. 2223–2232, Venice, Italy, October 2017.
- [14] O. Ronneberger, P. Fischer, and T. Brox, "U-net: convolutional networks for biomedical image segmentation," in *Proceedings of the International Conference on Medical Image Computing and Computer-Assisted Intervention*, pp. 234–241, Munich, Germany, October 2015.
- [15] M. Everingham and J. Winn, "The pascal visual object classes challenge 2012 (voc2012) development kit," in *Pattern Analysis, Statistical Modelling and Computational Learning*, Technical Report, Springer, Berlin, Germany, 2011.
- [16] M. Mirza and S. Osindero, "Conditional generative adversarial nets," 2014.
- [17] C. Ledig, L. Theis, F. Huszár et al., "Photo-realistic single image super-resolution using a generative adversarial network," in *Proceedings of the IEEE Conference on Computer Vision and Pattern Recognition*, pp. 4681–4690, Honolulu, HI, USA, July 2017.
- [18] C. Li and M. Wand, "Combining markov random fields and convolutional neural networks for image synthesis," in *Proceedings of the IEEE Conference on Computer Vision and Pattern Recognition*, pp. 2479–2486, Las Vegas, NV, USA, June 2016.